

Mass anomalous dimension in sextet QCD

Thomas DeGrand

Department of Physics, University of Colorado, Boulder, CO 80309, USA

Yigal Shamir and Benjamin Svetitsky

*Raymond and Beverly Sackler School of Physics and Astronomy,
Tel Aviv University, 69978 Tel Aviv, Israel*

We extend our previous study of the SU(3) gauge theory with $N_f = 2$ flavors of fermions in the sextet representation of color. Our tool is the Schrödinger functional method. By changing the lattice action, we push the bulk transition of the lattice theory to stronger couplings and thus reveal the beta function and the mass anomalous dimension γ_m over a wider range of coupling, out to $g^2 \simeq 11$. Our results are consistent with an infrared fixed point, but walking is not ruled out. Our main result is that γ_m never exceeds 0.45, making the model unsuitable for walking technicolor.

PACS numbers: 11.15.Ha, 11.10.Hi, 12.60.Nz

I. INTRODUCTION

For some time we have been studying SU(N) gauge theories with fermions in the symmetric two-index representation of color [1–6]. These are among the theories that have been proposed [7–9] as candidate models for walking technicolor [10–13]. Here we present our most recent work on the SU(3) gauge theory with $N_f = 2$ flavors of fermions in the sextet representation.

A technicolor theory must supply Goldstone bosons in order to generate masses for the weak vector bosons. To that end, the theory must break chiral symmetry spontaneously. In order to generate quark and lepton masses as well while avoiding large effects of flavor-changing neutral currents, one demands the additional property of *walking*. Here a large separation between the technicolor scale Λ_{TC} and the “extended” technicolor scale Λ_{ETC} is attained by having a near-zero of the beta function; the running coupling stalls for many decades in energy before chiral symmetry breaking sets in at large distances. Furthermore, the effect of the large ratio $\Lambda_{ETC}/\Lambda_{TC}$ on the technifermion condensate has to be enhanced by a large anomalous dimension γ_m of the mass operator $\bar{\psi}\psi$. Current estimates [14] require $\gamma_m \simeq 1$.

Since the beta function and γ_m are the important ingredients of walking technicolor, our work has focused on measuring them. We do this using Schrödinger-functional techniques [15–19], which are a lattice implementation of the background-field method. For other instances of the Schrödinger functional applied to technicolor candidates, see [20–26].

Our first effort [1] used Wilson’s fermion action with an added clover term [27] to reduce $O(a)$ effects, and was limited to lattices of linear size $L = 4a$ and $8a$. The result was a discrete beta function (DBF) that appeared to cross zero at a renormalized coupling $g^2 \simeq 2.0$, indicating an infrared fixed point (IRFP). An IRFP indi-

cates conformal physics at large distances, the antithesis of confinement. Intending to understand (and reduce) discretization effects, we then [4] went to larger lattices, $L/a = 6, 8, 12, 16$, and began using hypercubic smearing—fat links [28, 29]—in the fermion action. This work showed that the IRFP of Ref. [1] was but a lattice artifact. Thanks to its numerical stability, the fat-link action also enabled us to simulate at stronger couplings, out to $g^2 \simeq 4.6$, corresponding to a bare coupling $\beta = 4.4$. At stronger bare couplings we encountered a phase transition that makes it impossible to tune the hopping parameter κ so as to make the quark mass zero. The result of Ref. [4], then, is a beta function that is smaller in magnitude than the two-loop result but that does not cross zero in the accessible range of couplings.

In Ref. [4] we also calculated the anomalous dimension γ_m according to the method of [23, 30–32]. We found that γ_m first follows the one-loop curve but its rise slows at strong couplings so that $\gamma_m \lesssim 0.6$ in the range of couplings that we could reach.

In our current work on the SU(4) gauge theory with two-index (decuplet) fermions, which is still in progress [6], we encountered the same phase transition that prevents simulation of the massless theory. We found that augmenting the pure-gauge part of the action with a new fat-plaquette term can move this transition to stronger bare coupling and stronger renormalized coupling as well. In the present paper, we present the result of applying this strategy to the SU(3) theory. The new action enables us to reach $g^2 \simeq 11$, which is in the vicinity of the zero of the two-loop beta function, discussed by Caswell [33] and by Banks and Zaks [34]. We find that at this coupling our beta function as well has crossed zero. We can further state that the anomalous dimension has leveled off at $\gamma_m \lesssim 0.45$. We dismiss the earlier values near 0.6 as tainted by the nearby phase transition, which is after all a lattice artifact.

Because of statistical and systematic errors, the significance of the zero-crossing in the beta function leaves something to be desired. We claim, however, that the errors in γ_m are under control. Its small value near the fixed point, whether the latter is real or approximate (as desired for walking), spells trouble for any use of the present theory as walking technicolor.

Fodor *et al.* [35] have studied this theory by applying alternative scaling hypotheses to the mass spectrum as a function of the quark mass. Their conclusion favors confinement over conformal physics, meaning a QCD-like beta function without an IRFP. These authors have also published a more extensive analysis of SU(3) gauge theory coupled to twelve fundamental flavors [36], reaching similar conclusions for that theory. Their method for testing the hypothesis of (softly broken) conformality has been criticized in [37, 38].

Kogut and Sinclair [39–41] have been studying the present theory formulated with staggered fermions, attempting to distinguish confinement from conformality on the basis of movement of the chiral phase transition as the lattice size is changed. The results are so far inconclusive.

The plan of this paper is as follows. In Sec. II we present the improved lattice action, which is the only difference in the simulation method between this paper and Ref. [4]. For other details of our simulations we refer the reader to Ref. [4]. We also briefly discuss the ensembles we generated, and how we deal with the autocorrelations of our observables. We proceed in Sec. III to present our results for the running coupling and the beta function. Here we reanalyze the data of Ref. [4] according to the lights of our later paper on the SU(2) theory [5], where we learned to take advantage of the slow running in order to make maximum use of the several lattice sizes in play. Naturally, we add in the results of the new simulations obtained with the augmented gauge action. Section IV contains our results for the mass anomalous dimension γ_m , and we conclude with a brief summary in Sec. V.

II. LATTICE ACTION AND ENSEMBLES

Our action contains a fermion term and two pure gauge terms. The fermion term $\bar{\psi}D_F\psi$ is the conventional Wilson action, supplemented by a clover term [27] with coefficient $c_{\text{SW}} = 1$ [42]. The gauge links in the fermion action are fat link variables $V_\mu(x)$. The fat links are the normalized hypercubic (nHYP) links of Ref. [28], where for each link (x, μ) one takes the weighted average $V_\mu(x)$ of links in neighboring hypercubes with weights $\alpha_1 = 0.75$, $\alpha_2 = 0.6$, $\alpha_3 = 0.3$, reunitarized and subsequently promoted to the sextet representation.

The gauge action is

$$S_G = \frac{\beta}{2N} \sum_{\mu \neq \nu} \text{Re Tr } U_\mu(x) U_\nu(x + \hat{\mu}) U_\mu^\dagger(x + \hat{\nu}) U_\nu^\dagger(x)$$

$$+ \frac{\beta_f}{2d_f} \sum_{\mu \neq \nu} \text{Re Tr } V_\mu(x) V_\nu(x + \hat{\mu}) V_\mu^\dagger(x + \hat{\nu}) V_\nu^\dagger(x), \quad (1)$$

wherein the first term is the usual sum of plaquettes of fundamental thin link variables, while the second term contains plaquettes made of fat links in the sextet representation as in the fermion action. Here $N = 3$ is the number of colors while $d_f = 6$ is the dimension of the sextet. The weak-coupling expansion of S_G gives the effective bare coupling [6],

$$\frac{1}{g_0^2} = \frac{\beta}{2N} + \frac{T_f \beta_f}{d_f}, \quad (2)$$

where $T_f = 5/2$ is the group trace in the fermions' representation.¹

As before, we employ the hybrid Monte Carlo algorithm in our simulations. The molecular dynamics integration is accelerated with an additional heavy pseudo-fermion field as suggested by Hasenbusch [43], multiple time scales [44], and a second-order Omelyan integrator [45]. We determined the critical hopping parameter $\kappa_c = \kappa_c(\beta)$ by setting to zero the quark mass, obtained from the unimproved axial Ward identity on lattices of size $L = 12a$.

Without a systematic search, we found that choosing $\beta_f = +0.5$ removes the strong-coupling phase transition so that we can run at bare couplings down to $\beta = 2.0$; at smaller β the acceptance deteriorates rapidly, especially for larger volumes, so that we did not go far enough to find out if and where the strong-coupling transition turns up. At $\beta = 2.0$, the running coupling for $L = 6$ turns out to be $g^2 \simeq 11$. This is close to the two-loop Banks–Zaks zero at $g^2 = \frac{13}{194}(16\pi^2) \simeq 10.6$. We list in Table I the values of (β, κ_c) and the number of trajectories run at each volume, along with the length of the trajectories and the acceptance. Poor acceptance forced us to shorten the trajectory length in many cases from the usual value of 1.

The observables we measure are the (inverse) Schrödinger-functional running coupling, $1/g^2$, and the pseudoscalar renormalization factor, Z_P . (We measure Z_P on the same configurations used to determine $1/g^2$.) Both of them turn out to have long autocorrelations. We monitored and controlled this problem by running 4 or 8 streams in parallel at each β and L . After analyzing each stream separately, we fit the results of the streams together to a constant. We demanded that the χ^2/dof of the constant fit not exceed 6/3 for 4 streams, or 10/7 for 8 streams. For the largest volume $L = 16a$ at the strongest coupling $\beta = 2.0$, we were not able to overcome the autocorrelations in $1/g^2$ even with nearly 30,000 trajectories.

¹ We will present a test of weak-coupling universality in our forthcoming paper on the SU(4) theory.

TABLE I: Ensembles generated at the bare couplings (β, κ_c) for the lattice sizes L used in this study. Listed are the total number of trajectories for all streams at given (β, L) , the trajectory length, and the HMC acceptance.

β	κ_c	L/a	trajectories (thousands)	trajectory length	acceptance
3.5	0.13349	6	74.8	1.0	.93
		8	15.5	0.5	.97
		12	37.0	0.5	.88
2.5	0.13991	6	8.8	1.0	.61
		8	14.3	1.0	.43
		12	35.6	0.5	.50
		16	17.1	0.5	.48
2.0	0.14273	6	17.2	1.0	.65
		8	14.2	0.5	.61
		12	13.4	0.5	.48
		16	29.6	0.4	.38

We therefore omit this point from the analysis of the running coupling. The autocorrelations in Z_P , on the other hand, did allow a consistent determination, and thus we keep this point in the analysis of the mass anomalous dimension.

In this paper we present our new results, obtained with $\beta_f = 0.5$, alongside the $\beta_f = 0$ results presented in our earlier paper [4]. In the earlier study, we were less strict in controlling the autocorrelations. The main conclusions of this paper are derived exclusively from the new data.

III. BETA FUNCTION

The computation of the running coupling proceeds exactly as described in Ref. [4], with the same boundary conditions on the fermion and gauge fields. In brief, one imposes Dirichlet boundary conditions at the time slices $t = 0, L$, and measures the response of the quantum effective action. The coupling emerges from a measurement of the derivative of the action with respect to a parameter η in the boundary gauge field,

$$\frac{K}{g^2(L)} = \left\langle \frac{\partial S_G}{\partial \eta} - \text{tr} \left(\frac{1}{D_F^\dagger} \frac{\partial (D_F^\dagger D_F)}{\partial \eta} \frac{1}{D_F} \right) \right\rangle \Big|_{\eta=0}. \quad (3)$$

The constant K can be calculated directly from the classical continuum action. Only g_0 , Eq. (2), appears in the latter, which implies that $K = 12\pi$ regardless of β_f .

We presented in Ref. [4] the values of the running coupling g^2 for a number of values of (β, κ_c) with $\beta_f = 0$. Our new results for $\beta_f = 0.5$ are shown in Table II, and both sets are plotted in Fig. 1.²

TABLE II: Running coupling, Eq. (3), evaluated at the bare coupling (β, κ_c) with $\beta_f = 0.5$ on lattices of size L . For $\beta = 3.5$ we did not perform simulations with $L = 16$. The omission of the result for $L = 16$ at $\beta = 2.0$ is explained in the text.

β	$1/g^2$			
	$L = 6a$	$L = 8a$	$L = 12a$	$L = 16a$
3.5	0.2918(13)	0.2859(48)	0.2703(58)	–
2.5	0.1454(32)	0.1433(45)	0.1517(36)	0.1449(68)
2.0	0.0915(32)	0.1023(37)	0.1057(51)	*

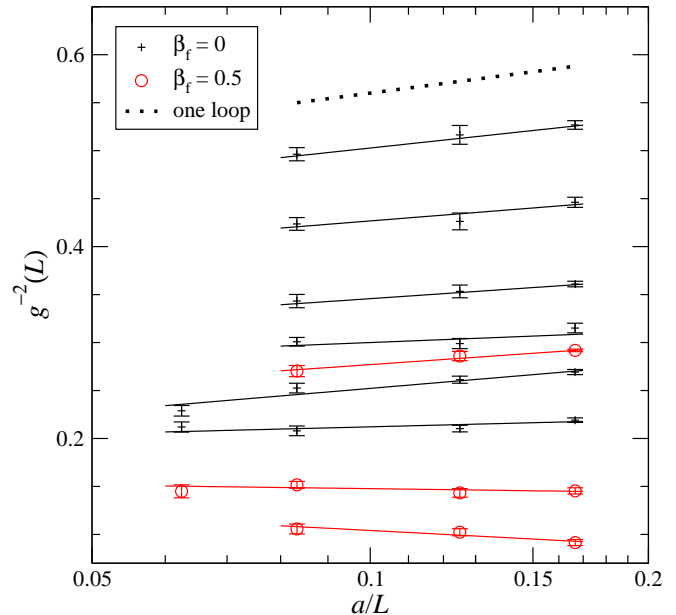


FIG. 1: Running coupling $1/g^2$ vs. a/L . The crosses are from simulations with $\beta_f = 0$ [4]: top to bottom, $\beta = 5.8, 5.4, 5.0, 4.8, 4.6$ and 4.4 . The circles are from simulations with $\beta_f = 0.5$ (Table II): top to bottom, $\beta = 3.5, 2.5$, and 2.0 . The straight lines are linear fits [Eq. (5)] to each set of points at given (β, β_f) ; the slope gives the beta function. The dotted line shows the expected slope from one-loop running.

It is convenient to define the beta function $\tilde{\beta}(u)$ for $u \equiv 1/g^2$ as

$$\tilde{\beta}(1/g^2) \equiv \frac{d(1/g^2)}{d \log L} = 2\beta(g^2)/g^4 = 2u^2\beta(1/u) \quad (4)$$

in terms of the conventional beta function $\beta(g^2)$. As discussed in Ref. [5], the slow running of the coupling justifies extracting the beta function at each (β, κ_c) from

² We have dropped from consideration the data obtained in [4] for

$(\beta, \beta_f) = (4.3, 0)$ since these were taken in a metastable state beyond the first-order boundary.

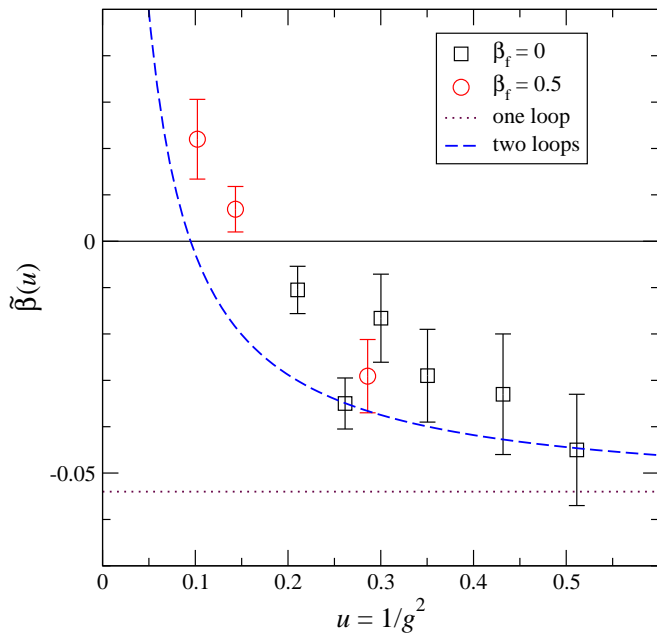


FIG. 2: Beta function $\tilde{\beta}(u)$ as extracted from the linear fits (5), plotted as a function of $u(L = 8a)$. The squares are from the $\beta_f = 0$ data while the circles are from $\beta_f = 0.5$. Plotted curves are the one-loop (dotted line) and two-loop (dashed line) beta functions.

a linear fit of the inverse coupling

$$u(L/a) = c_0 + c_1 \log \frac{L}{8a}. \quad (5)$$

With this parametrization, c_0 gives the inverse coupling $u(L = 8a)$, while c_1 is an estimate for the beta function β at this coupling. These fits are shown in Fig. 1. Each fit was done using all the available volumes at the given bare parameters. Values of the beta function $\tilde{\beta}(u)$ obtained from these fits are plotted as a function of $u(L = 8a)$ in Fig. 2. One can see that the results for $\beta_f = 0$ and for $\beta_f = 0.5$ are consistent with each other. Also shown are the one- and two-loop approximations from the expansion

$$\tilde{\beta}(u) = -\frac{2b_1}{16\pi^2} - \frac{2b_2}{(16\pi^2)^2} \frac{1}{u} + \dots, \quad (6)$$

where $b_1 = 13/3$ and $b_2 = -194/3$.

The assumption behind the linear fits is that $\tilde{\beta}$ is small so that $u(L/a)$ changes very slowly with the volume; this behavior is apparent in Fig. 1. Indeed the fits have good χ^2 , which justifies our hypothesis. Corrections to the simple model (5) come from discretization errors, as well as from the slight deviation from constancy of the continuum beta function over the range of volumes. Discretization errors have the form of powers of a/L . We have found that such corrections are only loosely constrained in a generalized fit; thus we prefer to estimate the uncertainty due to these corrections by redoing the

TABLE III: Pseudoscalar renormalization factor Z_P evaluated at the couplings (β, κ_c) , with $\beta_f = 0.5$, for lattice sizes L .

β	Z_P			
	$L = 6a$	$L = 8a$	$L = 12a$	$L = 16a$
3.5	0.2171(2)	0.1923(8)	0.1680(5)	—
2.5	0.1787(4)	0.1560(5)	0.1325(6)	0.1192(8)
2.0	0.1579(6)	0.1371(6)	0.1183(10)	0.1024(10)

linear fits while omitting the smallest lattice, $L = 6a$. The results are shown in the left-hand panel of Fig. 3. While the error bars have increased, on the whole the results are stable.³

Deviations from constancy of the (continuum) beta function give rise to higher powers of $\log L/a$. Adding the next-to-leading term, at each bare coupling we fit

$$u(L/a) = c_0 + c_1 \log L/8a + c_2 (\log L/8a)^2. \quad (7)$$

From the definition of the beta function it follows that c_1 continues to provide an estimate for the beta function at $u = 1/g^2(L = 8a)$. The results of these fits are shown in the right-hand panel of Fig. 3. Once again, there is only a small change compared to the linear fits of Eq. (5).⁴

At the two strongest couplings the beta function is positive, indicating the existence of an infrared fixed point g_* . For each fit type, we determine the zero of the beta function from a linear fit of $\tilde{\beta}$ vs. u , using only the three $\beta_f = 0.5$ points. The value of $u_* = 1/g_*^2$ obtained from the linear fits with all volumes included is 0.172(15), while when $L = 6a$ is omitted we obtain 0.159(29). The result for the fits of the form (7) is 0.184(17). Taking as our combined (statistical and systematic) uncertainty the union of the 1σ intervals, we arrive at⁵

$$5 \leq g_*^2 \leq 7.5. \quad (8)$$

The assumption of a linear zero of the beta function gives a consistent estimate of its location for all fit types. This assumption, however, can be questioned. If we consider the beta function obtained from the linear fits with the smallest volumes omitted (Fig. 3, left panel), we see that it is possible that the beta function remains negative even at the strongest couplings studied. Hence, we cannot rule out a “walking” scenario wherein the beta function comes close to zero, but never actually turns positive.

³ Note that dropping $L = 6a$ for the cases where there are only three volumes leaves no degrees of freedom for the linear fit.

⁴ Here, too, fitting the cases with only three volumes leaves no degrees of freedom for the fit.

⁵ These fits, as well as similar fits in which one or two $\beta_f = 0$ points are added, all have good χ^2 . The fit results with the added $\beta_f = 0$ points agree with Eq. (8).

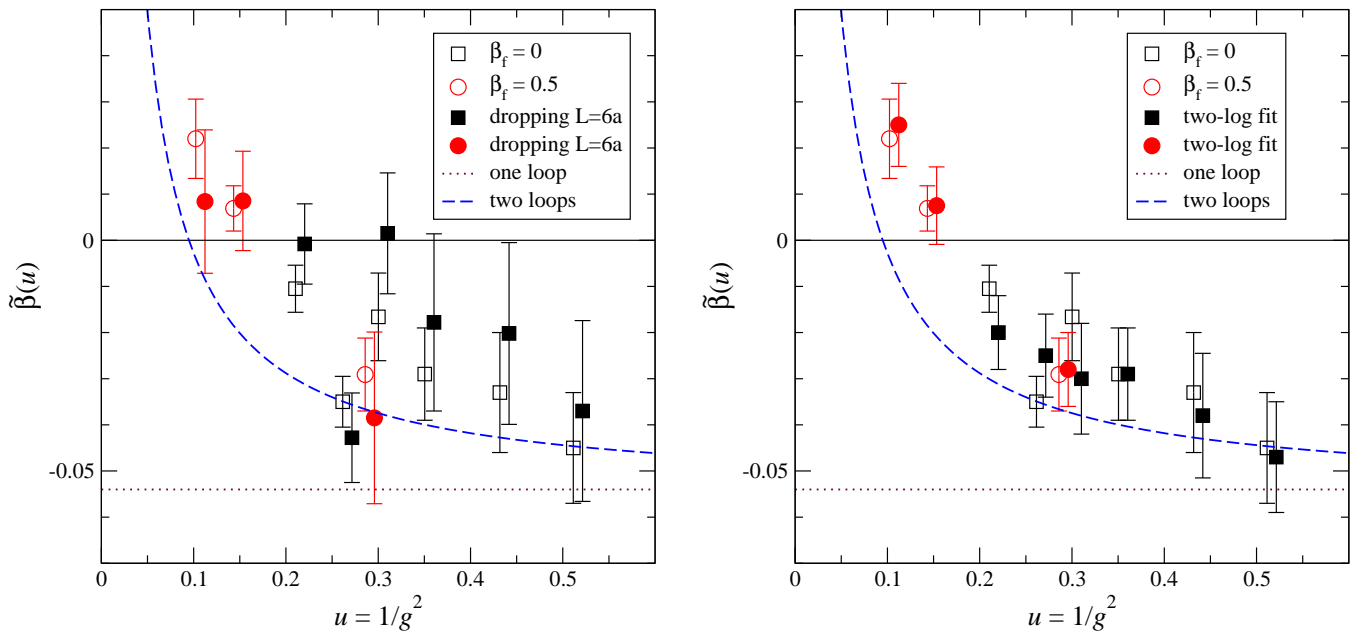


FIG. 3: Comparison of different fit types. Empty symbols as in Fig. 2. Left panel: full symbols derive from linear fits in which the $L = 6a$ points are omitted. Right panel: full symbols derive from fits to Eq. (7), in which a \log^2 term has been added. Results are plotted against $u(L = 8a)$. The filled symbols have been slightly displaced to the right.

In the next section, we will show that, despite this uncertainty, the behavior of the mass anomalous dimension make this theory unsuitable for models of walking technicolor.

IV. MASS ANOMALOUS DIMENSION

We derive the mass anomalous dimension from the scaling with L of the pseudoscalar renormalization factor Z_P . The latter is calculated by taking the ratio

$$Z_P = \frac{c\sqrt{f_1}}{f_P(L/2)}. \quad (9)$$

f_P is the propagator from the a wall source at the $t = 0$ boundary to a point pseudoscalar operator at time $L/2$. The normalization of the wall source is removed by the f_1 factor, which is a boundary-to-boundary correlator. The constant c , which is an arbitrary normalization, is $1/\sqrt{2}$ in our convention.

We present in Table III the results of calculating Z_P in our runs with $\beta_f = 0.5$; we plot them, together with the $\beta_f = 0$ results [4], in Fig. 4. Again, the slow running suggests that we may attempt to extract γ_m from the approximate scaling formula

$$Z_P(L) = Z_P(L_0) \left(\frac{L_0}{L} \right)^\gamma, \quad (10)$$

that is, from the slopes of the lines drawn in Fig. 4. These

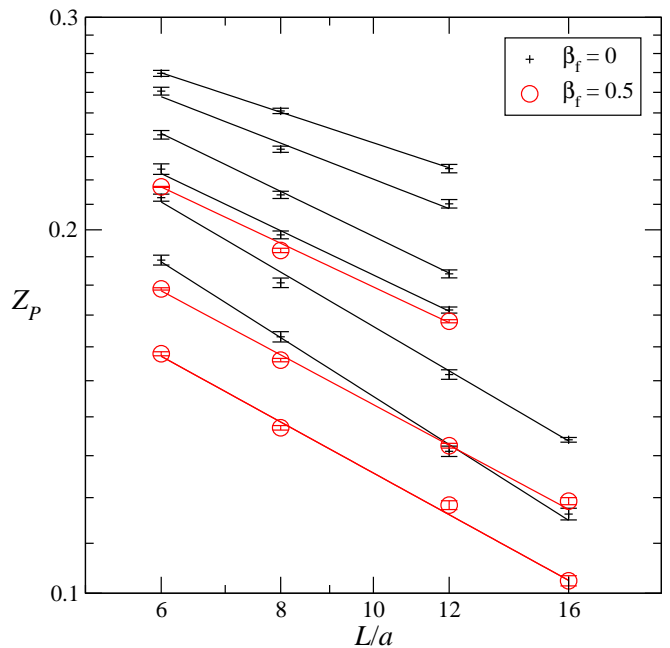


FIG. 4: The pseudoscalar renormalization constant Z_P vs. L/a . The crosses are from simulations with $\beta_f = 0$, $\beta = 5.8$ to 4.4 . The circles are from simulations with $\beta_f = 0.5$ (Table III): top to bottom, $\beta = 3.5$, 2.5 , and 2.0 . The straight lines are fits to each set of points at given (β, β_f) ; the slope gives γ_m .

linear fits are analogous to Eq. (5):

$$\log Z_P(L/a) = c_0 + c_1 \log \frac{L}{8a}. \quad (11)$$

The results are shown in Fig. 5. Similarly, we have also applied the linear fit with the smallest volume $L = 6a$ removed, and we considered a fit function analogous to Eq. (7),

$$\log Z_P(L/a) = c_0 + c_1 \log L/8a + c_2(\log L/8a)^2. \quad (12)$$

In all cases the mass anomalous dimension at $g^2(L = 8a)$ is given by $-c_1$. We show a comparison of the different fit types in Fig. 5, plotted against the running coupling $g^2(L = 8a)$. It is apparent that the result for $\gamma_m(g^2)$ is quite robust under variations in the fitting procedure. The quality of the fits will be discussed shortly.

A comparison of the new data to the old shows that there is some disagreement. Of the three points obtained with $\beta_f = 0.5$, only the weakest-coupling point is in agreement with the results of $\beta_f = 0$ simulations. The two strongest-coupling points obtained with $\beta_f = 0$ lie far above the line connecting the $\beta_f = 0.5$ points. The former originate from simulations near the strong-coupling transition of the $\beta_f = 0$ theory. This is a lattice artifact, pushed off to stronger couplings by the introduction of $\beta_f > 0$. Thus the disagreement between the two sets of results should be settled in favor of the new results, leading us in effect to abandon the last two points in the old set.

The linear fits to $Z_P(L/a)$ that include all volumes have high χ^2 for all three $\beta_f = 0.5$ points. (See Table IV. This is apparent in Fig. 4.) Let us discuss them one by one.

1. At the weakest-coupling point of the $\beta_f = 0.5$ data set, obtained at $\beta = 3.5$, we have only three volumes. Dropping the smallest volume leaves zero degrees of freedom in the linear fit, so that there is really no alternative to the all-volume fit. As can be seen, however, the latter gives a value of γ_m in good agreement with the $\beta_f = 0.0$ data set, and both lie close to the one-loop curve. The $\beta_f = 0.0$ fits *do* have good χ^2 . Given the agreement of the two data sets in this case, we decided that it is unnecessary to carry out $L = 16a$ simulations at $(\beta, \beta_f) = (3.5, 0.5)$.
2. Next: At $(\beta, \beta_f) = (2.5, 0.5)$, when the smallest volume is dropped, the linear fit has good χ^2 . Notice that this is the point that lies inside the range that we have determined for g_*^2 in the previous section. Indeed at a fixed point Eq. (10) should become exact in the infrared.
3. Finally, for $(\beta, \beta_f) = (2.0, 0.5)$ all fits have high χ^2 . Nevertheless, the robustness of the result when changing the fit type makes it unlikely that the true value of γ_m could be very different.

All our fits show that γ_m departs from the one-loop line and levels off at strong coupling.

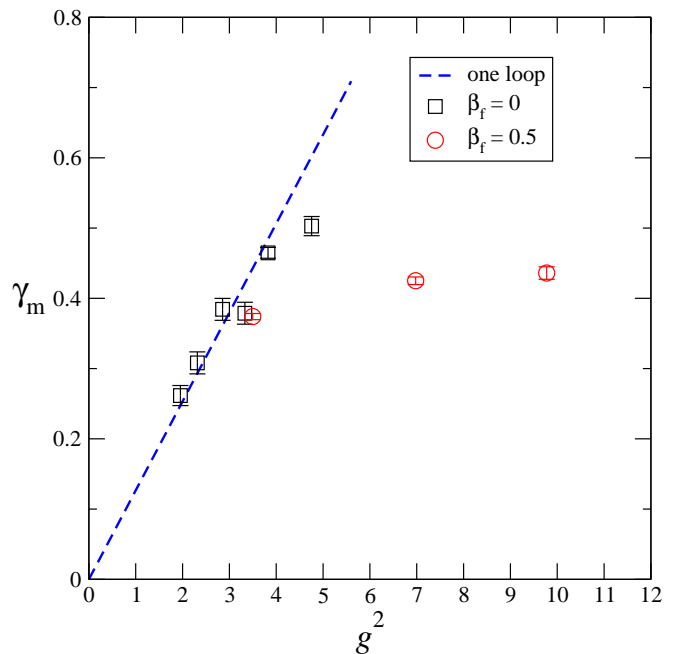


FIG. 5: Mass anomalous dimension $\gamma_m(g^2)$ from the linear fits shown in Fig. 4, plotted against $g^2(L = 8a)$. The squares are from the $\beta_f = 0$ data while the circles are from $\beta_f = 0.5$. The line is the one-loop result.

TABLE IV: Quality of fits for γ_m .

β	χ^2/dof		
	Eq. (11)	dropping $L = 6a$	Eq. (12)
3.5	11/1	—	—
2.5	18/2	0.9/1	0.4/1
2.0	12/2	5/1	9/1

V. SUMMARY

In this paper we have continued our study of the SU(3) gauge theory with two flavors of sextet fermions. A new term in the lattice action allowed us to explore a much wider range of the renormalized coupling. The old and new actions give rise to consistent results for the beta function where they overlap. For the mass anomalous dimension there are some disagreements. The results obtained using the new action must be favored over the old ones, as the source of the disagreement must be the proximity of the first-order phase transitions—a lattice artifact—in the old action.

Our results for the running coupling are consistent with the existence of an infrared fixed point in the range $5 \leq g_*^2 \leq 7.5$. Nonetheless, in contrast to our SU(2) study [5], where our strongest-coupling point in the beta function was positive by at least 6σ , none of the strong-coupling

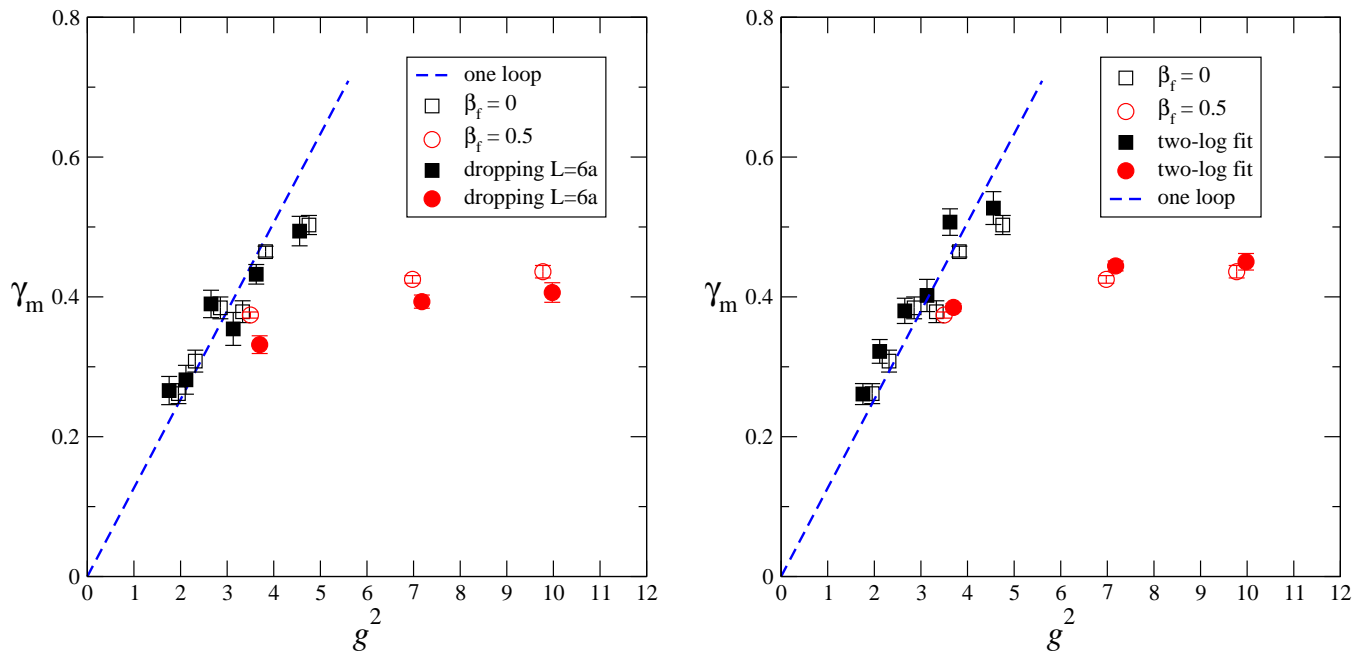


FIG. 6: Comparison of different fit types. Empty symbols as in Fig. 5. Left panel: full symbols derive from linear fits in which the $L = 6a$ points are omitted. Right panel: full symbols derive from fits to Eq. (7), in which a \log^2 term has been added. Results are plotted against $g^2(L = 8a)$. The filled symbols have been slightly displaced horizontally.

points here are positive by more than 2.5σ , and in the worst case (dropping $L = 6$), none are positive by more than 1σ . Thus a “walking” scenario is not ruled out.

As in the $SU(2)$ theory, γ_m first follows the one-loop curve, but when it reaches a value $\gamma_m \approx 0.4$ it levels off. The value of γ_m at the fixed point g_* , if this fixed point exists, is scheme-independent. We can go beyond this, however. Throughout the entire range studied, the mass anomalous dimension is bounded from above,

$$\gamma_m \lesssim 0.45. \quad (13)$$

Such a bound is evidently invariant under any redefinition $g \rightarrow g'(g)$, and hence our bound is entirely scheme-independent.

A successful model of walking (extended) technicolor must have a slowly-varying coupling, but no infrared fixed point; it must also have a large mass anomalous dimension, $\gamma_m \simeq 1$. While our results do not rule out walking in the sextet theory, the smallness of γ_m makes this theory unsuitable for walking technicolor.

Acknowledgments

B. S. and Y. S. thank the University of Colorado for hospitality. This work was supported in part by the Israel Science Foundation under grant no. 423/09 and by the U. S. Department of Energy.

The computations for this research were made possible in part by the U. S. National Science Foundation through TeraGrid resources provided by (1) the University of Texas and (2) the National Institute for Computational Sciences (NICS) at the University of Tennessee, under grant number TG-PHY090023. Additional computations were done on facilities of the USQCD Collaboration at Fermilab, which are funded by the Office of Science of the U. S. Department of Energy. Our computer code is based on the publicly available package of the MILC collaboration [46]. The code for hypercubic smearing was adapted from a program written by A. Hasenfratz, R. Hoffmann and S. Schaefer [47].

-
- [1] Y. Shamir, B. Svetitsky and T. DeGrand, *Zero of the discrete beta function in $SU(3)$ lattice gauge theory with color sextet fermions*, Phys. Rev. D **78**, 031502 (2008) [arXiv:0803.1707 [hep-lat]].
- [2] T. DeGrand, Y. Shamir and B. Svetitsky, *Phase structure of $SU(3)$ gauge theory with two flavors of symmetric-*

representation fermions, Phys. Rev. D **79**, 034501 (2009) [arXiv:0812.1427 [hep-lat]].

- [3] T. DeGrand, *Finite-size scaling tests for $SU(3)$ lattice gauge theory with color sextet fermions*, Phys. Rev. D **80**, 114507 (2009) [arXiv:0910.3072 [hep-lat]].
- [4] T. DeGrand, Y. Shamir, B. Svetitsky, *Running coupling*

- and mass anomalous dimension of $SU(3)$ gauge theory with two flavors of symmetric-representation fermions, Phys. Rev. D **82**, 054503 (2010). [arXiv:1006.0707 [hep-lat]].
- [5] T. DeGrand, Y. Shamir, B. Svetitsky, *Infrared fixed point in $SU(2)$ gauge theory with adjoint fermions*, Phys. Rev. D **83**, 074507 (2011). [arXiv:1102.2843 [hep-lat]].
- [6] T. DeGrand, Y. Shamir, B. Svetitsky, *Gauge theories with fermions in the two-index symmetric representation*, [arXiv:1110.6845 [hep-lat]].
- [7] F. Sannino and K. Tuominen, *Orientifold theory dynamics and symmetry breaking*, Phys. Rev. D **71**, 051901 (2005) [arXiv:hep-ph/0405209].
- [8] D. K. Hong, S. D. H. Hsu and F. Sannino, *Composite Higgs from higher representations*, Phys. Lett. B **597**, 89 (2004) [arXiv:hep-ph/0406200].
- [9] D. D. Dietrich, F. Sannino and K. Tuominen, *Light composite Higgs from higher representations versus electroweak precision measurements: Predictions for LHC*, Phys. Rev. D **72**, 055001 (2005) [arXiv:hep-ph/0505059].
- [10] C. T. Hill and E. H. Simmons, *Strong dynamics and electroweak symmetry breaking*, Phys. Rept. **381**, 235 (2003) [Erratum-ibid. **390**, 553 (2004)] [arXiv:hep-ph/0203079].
- [11] B. Holdom, *Raising The Sideways Scale*, Phys. Rev. D **24**, 1441 (1981).
- [12] K. Yamawaki, M. Bando and K. i. Matumoto, *Scale Invariant Technicolor Model And A Technidilaton*, Phys. Rev. Lett. **56**, 1335 (1986).
- [13] T. Appelquist, J. Terning and L. C. R. Wijewardhana, *Postmodern technicolor*, Phys. Rev. Lett. **79**, 2767 (1997) [arXiv:hep-ph/9706238].
- [14] R. S. Chivukula and E. H. Simmons, *Condensate enhancement and D -meson mixing in technicolor theories*, Phys. Rev. D **82**, 033014 (2010) [arXiv:1005.5727 [hep-lat]].
- [15] M. Lüscher, R. Narayanan, P. Weisz and U. Wolff, *The Schrödinger functional: A Renormalizable probe for non-Abelian gauge theories*, Nucl. Phys. B **384**, 168 (1992) [arXiv:hep-lat/9207009].
- [16] M. Lüscher, R. Sommer, P. Weisz and U. Wolff, *A precise determination of the running coupling in the $SU(3)$ Yang-Mills theory*, Nucl. Phys. B **413**, 481 (1994) [arXiv:hep-lat/9309005].
- [17] S. Sint and R. Sommer, *The running coupling from the QCD Schrödinger functional: A one loop analysis*, Nucl. Phys. B **465**, 71 (1996) [arXiv:hep-lat/9508012].
- [18] K. Jansen and R. Sommer [ALPHA collaboration], *$O(\alpha)$ improvement of lattice QCD with two flavors of Wilson quarks*, Nucl. Phys. B **530**, 185 (1998) [Erratum-ibid. B **643**, 517 (2002)] [arXiv:hep-lat/9803017].
- [19] M. Della Morte et al. [ALPHA Collaboration], *Computation of the strong coupling in QCD with two dynamical flavours*, Nucl. Phys. B **713**, 378 (2005) [arXiv:hep-lat/0411025].
- [20] T. Appelquist, G. T. Fleming and E. T. Neil, *Lattice study of the conformal window in QCD-like theories*, Phys. Rev. Lett. **100**, 171607 (2008) [Erratum-ibid. **102**, 149902 (2009)] [arXiv:0712.0609 [hep-ph]].
- [21] T. Appelquist, G. T. Fleming and E. T. Neil, *Lattice Study of Conformal Behavior in $SU(3)$ Yang-Mills Theories*, Phys. Rev. D **79**, 076010 (2009) [arXiv:0901.3766 [hep-ph]].
- [22] A. J. Hietanen, K. Rummukainen and K. Tuominen, *Evolution of the coupling constant in $SU(2)$ lattice gauge theory with two adjoint fermions*, Phys. Rev. D **80**, 094504 (2009) [arXiv:0904.0864 [hep-lat]].
- [23] F. Bursa, L. Del Debbio, L. Keegan, C. Pica and T. Pickup, *Mass anomalous dimension in $SU(2)$ with two adjoint fermions*, Phys. Rev. D **81**, 014505 (2010) [arXiv:0910.4535 [hep-ph]].
- [24] F. Bursa, L. Del Debbio, L. Keegan, C. Pica and T. Pickup, *Mass anomalous dimension in $SU(2)$ with six fundamental fermions*, Phys. Lett. B **696**, 374 (2011) [arXiv:1007.3067 [hep-ph]].
- [25] M. Hayakawa, K. -I. Ishikawa, Y. Osaki, S. Takeda, S. Uno and N. Yamada, *Running coupling constant of ten-flavor QCD with the Schrödinger functional method*, Phys. Rev. D **83**, 074509 (2011) [arXiv:1011.2577 [hep-lat]].
- [26] T. Karavirta, J. Rantaharju, K. Rummukainen and K. Tuominen, *Determining the conformal window: $SU(2)$ gauge theory with $N_f = 4, 6$ and 10 fermion flavours*, arXiv:1111.4104 [hep-lat].
- [27] B. Sheikholeslami and R. Wohlert, *Improved continuum limit lattice action for QCD with Wilson fermions*, Nucl. Phys. B **259**, 572 (1985).
- [28] A. Hasenfratz and F. Knechtli, *Flavor symmetry and the static potential with hypercubic blocking*, Phys. Rev. D **64**, 034504 (2001) [arXiv:hep-lat/0103029].
- [29] A. Hasenfratz, R. Hoffmann and S. Schaefer, *Hypercubic smeared links for dynamical fermions*, JHEP **0705**, 029 (2007) [arXiv:hep-lat/0702028].
- [30] S. Sint and P. Weisz [ALPHA collaboration], *The running quark mass in the SF scheme and its two-loop anomalous dimension*, Nucl. Phys. B **545**, 529 (1999) [arXiv:hep-lat/9808013].
- [31] S. Capitani, M. Lüscher, R. Sommer and H. Wittig [ALPHA Collaboration], *Non-perturbative quark mass renormalization in quenched lattice QCD*, Nucl. Phys. B **544**, 669 (1999) [arXiv:hep-lat/9810063].
- [32] M. Della Morte et al. [ALPHA Collaboration], *Non-perturbative quark mass renormalization in two-flavor QCD*, Nucl. Phys. B **729**, 117 (2005) [arXiv:hep-lat/0507035].
- [33] W. E. Caswell, *Asymptotic behavior of nonabelian gauge theories to two loop order*, Phys. Rev. Lett. **33**, 244 (1974).
- [34] T. Banks and A. Zaks, *On the phase structure of vector-like gauge theories with massless fermions*, Nucl. Phys. B **196**, 189 (1982).
- [35] Z. Fodor, K. Holland, J. Kuti, D. Nógrádi and C. Schroeder, *Chiral symmetry breaking in fundamental and sextet fermion representations of $SU(3)$ color*, arXiv:1103.5998 [hep-lat].
- [36] Z. Fodor, K. Holland, J. Kuti, D. Nógrádi, and C. Schroeder, *Twelve massless flavors and three colors below the conformal window*, Phys. Lett. B **703**, 348 (2011) [arXiv:1104.3124 [hep-lat]].
- [37] T. Appelquist, G. T. Fleming, M. F. Lin, E. T. Neil and D. A. Schaich, *Lattice Simulations and Infrared Conformality*, Phys. Rev. D **84**, 054501 (2011) [arXiv:1106.2148 [hep-lat]].
- [38] T. DeGrand, *Finite-size scaling tests for spectra in $SU(3)$ lattice gauge theory coupled to 12 fundamental flavor fermions*, Phys. Rev. D **84**, 116901 (2011) [arXiv:1109.1237 [hep-lat]].
- [39] J. B. Kogut and D. K. Sinclair, *Thermodynamics of lattice QCD with 2 flavours of colour-sextet quarks: A*

- model of walking/conformal Technicolor*, Phys. Rev. D **81**, 114507 (2010) [arXiv:1002.2988 [hep-lat]].
- [40] J. B. Kogut and D. K. Sinclair, *Thermodynamics of lattice QCD with 2 sextet quarks on $N_t=8$ lattices*, Phys. Rev. D **84**, 074504 (2011) [arXiv:1105.3749 [hep-lat]].
- [41] D. K. Sinclair and J. B. Kogut, *The chiral phase transition for QCD with sextet quarks*, arXiv:1111.2319 [hep-lat].
- [42] Y. Shamir, B. Svetitsky, E. Yurkovsky, *Improvement via hypercubic smearing in triplet and sextet QCD*, Phys. Rev. **D83**, 097502 (2011). [arXiv:1012.2819 [hep-lat]].
- [43] M. Hasenbusch, *Speeding up the Hybrid-Monte-Carlo algorithm for dynamical fermions*, Phys. Lett. B **519**, 177 (2001) [arXiv:hep-lat/0107019].
- [44] C. Urbach, K. Jansen, A. Shindler and U. Wenger, *HMC algorithm with multiple time scale integration and mass preconditioning*, Comput. Phys. Commun. **174**, 87 (2006) [arXiv:hep-lat/0506011].
- [45] T. Takaishi and P. de Forcrand, *Testing and tuning new symplectic integrators for hybrid Monte Carlo algorithm in lattice QCD*, Phys. Rev. E **73**, 036706 (2006) [arXiv:hep-lat/0505020].
- [46] <http://www.physics.utah.edu/~detar/milc/>
- [47] A. Hasenfratz, R. Hoffmann and S. Schaefer, *Low energy chiral constants from epsilon-regime simulations with improved Wilson fermions*, Phys. Rev. D **78**, 054511 (2008) [arXiv:0806.4586 [hep-lat]].